In Vitro and In Vivo Optimization of Infrared Laser Treatment for Injured Peripheral Nerves

Juanita J. Anders, PhD,[1*] Helina Moges, BS,[1] Xingjia Wu, BS,[1] Isaac D. Erbele, MD,[1] Stephanie L. Alberico, BS,[1] Edward K. Saidu, BS,[1] Jason T. Smith, PhD,[2] and Brian A. Pryor, PhD[2]

[1]*Department of Anatomy, Physiology and Genetics, Uniformed Services University of the Health Sciences, 4301 Jones Bridge Road, Bethesda, Maryland 20814*

[2]*LiteCure LLC, 250 Corporate Blvd, STE B, Newark, Delaware 19702*

Background and Objective: Repair of peripheral nerve injuries remains a major challenge in restorative medicine. Effective therapies that can be used in conjunction with surgical nerve repair to improve nerve regeneration and functional recovery are being actively investigated. It has been demonstrated by a number of peer reviewed publications that photobiomodulation (PBM) supports nerve regeneration, reinnervation of the denervated muscle, and functional recovery after peripheral nerve injury. However, a key issue in the use of PBM as a treatment for peripheral nerve injury is the lack of parameter optimization for any given wavelength. The objective of this study was to demonstrate that for a selected wavelength effective *in vitro* dosing parameters could be translated to effective *in vivo* parameters.

Materials and Methods: Comparison of infra-red (810 and 980 nm wavelengths) laser treatment parameters for injured peripheral nerves was done beginning with a series of *in vitro* experiments using primary human fibroblasts and primary rat cortical neurons. The primary rat cortical neurons were used for further optimization of energy density for 980 nm wavelength light using measurement of total neurite length as the bioassay. For these experiments, the parameters included a 1 W output power, power density of 10 mW/cm^2, and energy densities of 0.01, 0.1, 0.5, 2, 10, 50, 200, 1,000, and 5,000 mJ/cm^2. For translation of the *in vitro* data for use *in vivo* it was necessary to determine the transcutaneous penetration of 980 nm wavelength light to the level of the peroneal nerve. Two anesthetized, male White New Zealand rabbits were used for these experiments. The output power of the laser was set at 1.0 or 4.0 W. Power density measurements were taken at the surface of the skin, sub-dermally, and at the level of the nerve. Laser parameters used in the *in vivo* studies were calculated based on data from the *in vitro* studies and the light penetration measurements. For the *in vivo* experiments, a total of 22 White New Zealand rabbits (2.34–2.89 kg) were used. Translated dosing parameters were refined in a pilot study using a transection model of the peroneal nerve in rabbits. Output powers of 2 and 4 W were tested. For the final set of *in vivo* experiments, the same transection nerve injury model was used. An energy density of 10 mW/cm^2 at the level of the peroneal nerve was selected and the laser parameters were further refined. The dosing parameters used were: 1.5 W output power, 43 seconds exposure, 8 cm^2 area and a total energy of 65 J.

Results: In vitro, 980 nm wavelength light at 10 mW/cm^2 significantly improved neurite elongation at energy densities between 2 and 200 mJ/cm^2. In vivo penetration of the infrared light measured in anesthetized rabbits showed that on average, 2.45% of the light applied to the skin reached the depth of the peroneal nerve. The *in vivo* pilot study data revealed that the 4 W parameters inhibited nerve regeneration while the 2 W parameters significantly improved axonal regrowth. For the final set of experiments, the irradiated group performed significantly better in the toe spread reflex test compared to the control group from week 7 post-injury, and the average length of motor endplates returned to uninjured levels.

Conclusion: The results of this study demonstrate that treatment parameters can be determined initially using *in vitro* models and then translated to *in vivo* research and clinical practice. Furthermore, this study establishes that infrared light with optimized parameters promotes accelerated nerve regeneration and improved functional recovery in a surgically repaired peripheral nerve. Lasers Surg. Med. © 2013 Wiley Periodicals, Inc.

Key words: immunolabeling; light therapy; motor end plates; peripheral nerve injury; photobiomodulation; regeneration; re-innervation; toe spread reflex

"Conflict of Interest Disclosures: All authors have completed and submitted the ICMJE Form for Disclosure of Potential Conflicts of Interest and none were reported."

Contract grant sponsor: Comprehensive National Neuroscience Program; Contract grant number: #G1704T.

*Correspondence to: Juanita J. Anders, PhD, Department of Anatomy, Physiology and Genetics, Uniformed Services University of the Health Sciences, 4301 Jones Bridge Road, Bethesda, MD 20814. E-mail: juanita.anders@usuhs.edu

Accepted 19 November 2013

Published online in Wiley Online Library (wileyonlinelibrary.com).

DOI 10.1002/lsm.22212

INTRODUCTION

Post-traumatic repair of peripheral nerve injuries remains a major challenge in restorative medicine. In the United States, 50,000 peripheral nerve repair procedures are performed annually [1]. Although major advances have been made in the microsurgical repair of injured peripheral nerves [2], clinical results and functional recovery have been disappointing [3,4]. The current challenge is to identify effective therapies that can be used in conjunction with surgical nerve repair to improve nerve regeneration and functional recovery.

There is an impressive number of peer reviewed publications on the treatment of peripheral nerve injury with photobiomodulation (PBM). Based on reviews of this literature, PBM supports peripheral nerve regeneration, reinnervation of the denervated muscle, and functional recovery after peripheral nerve injury [5–7]. However, a key issue in the use of PBM as a treatment for peripheral nerve injury is the lack of parameter optimization for any given wavelength. Selection of treatment parameters was often based on published reports or transfer of parameters from other studies in the laboratory or clinic. Preliminary studies to optimize the treatment parameters were rarely done.

Review of this literature also underscores that many wavelengths can support peripheral nerve injury repair. The wavelengths primarily used in these studies ranged in the 600–904 nm range [6,7]. Wavelength selection was also often based on devices available to the laboratory or clinic, published reports, or transfer of wavelength selection to peripheral nerve injury studies from *in vivo* or *in vitro* experiments on other types of injuries.

Successful therapeutic use of any particular wavelength requires penetration to the target tissue and treatment parameters that can deliver a therapeutic dose at the tissue. Currently many available laser devices used for PBM emit at least a percentage of 980 nm wavelength light (personal communication with Dr. Smith). However, there are no published reports on optimization of parameters for this wavelength. Therefore, 980 nm wavelength light was chosen for this study. The objective of this study was to demonstrate that for a selected wavelength effective *in vitro* dosing parameters could be translated to effective *in vivo* use. A systematic approach was taken for optimization of treatment parameters beginning with a series of *in vitro* cellular models including primary human fibroblasts and rat cortical neurons. For the primary human fibroblasts, laser parameter optimization was initially done with 810 nm wavelength light. We previously reported that 810 nm wavelength light at several combinations of power density and treatment time supported differentiation of normal human neural progenitor cells *in vitro* [8]. We were interested in determining if these same optimized combinations of power density and time for 810 nm wavelength light could have a photobiomodulatory effect on a different cell type, the primary human fibroblast, and measured by a different bioassay, mitochondrial metabolism. Once the effective combinations of power density and time for the 810 nm wavelength light were identified for the primary human fibroblasts, these same combinations were tested using 980 nm wavelength light. The *in vitro* studies were then expanded to include further optimization of the 980 nm wavelength light using rat cortical neurons. In vivo penetration measurements of 980 nm wavelength light to the depth of the peroneal nerve were done to aid in the translation of the *in vitro* optimized parameters for use *in vivo*. An *in vivo* pilot study was then conducted to refine the dosing parameters followed by a definitive test of the optimized parameters based on behavioral and immunohistological analyses.

The results of this study demonstrate that treatment parameters can be determined initially using *in vitro* models and then translated to animal model research and clinical practice. Furthermore, this study establishes that infrared light with optimized parameters promotes accelerated nerve regeneration and improved functional recovery in a surgically repaired peripheral nerve.

MATERIALS AND METHODS

In Vitro Experiments: Initial Optimization of Laser Parameters using In Vitro Human Fibroblasts and Rat Cortical Neurons

Culture of primary human fibroblasts. Primary human fibroblasts (ATCC, Manassas, VA) were cultured in DMEM with 10% fetal bovine serum (FBS) and 4.5 g/L D-glucose. After trypsinization, 5×10^3 cells were seeded per well in a 24-well plate with DMEM containing 2% FBS and 1 g/L D-glucose. The fibroblasts were allowed to attach by incubating for 1 hour at 37°C, 5% CO_2 before irradiation.

Laser irradiation of primary human fibroblasts. After attachment to the substrate, fibroblasts were exposed to light with a wavelength of 810 or 980 nm. A continuous wave (CW) 810 nm diode laser (Thor International, Chesham, UK; 200 mW output, modified and homogenized with a delivery optical fiber resulting in an output power of 150 mW) was used. A 980 nm CW laser (LiteCure, LLC, Newark, DE; Model No. PLT-980–10; output power: 1 to 10 W) was used at 1 W output power. A power density of 10 mW/cm^2 and energy densities of 200, 1,000, or 5,000 mJ/cm^2 were used for both lasers. Six out of 24 wells in each culture plate were seeded in a group of two adjacent wells. The height of laser above the plate was adjusted to attain an energy density of 10 mW/cm^2 and to irradiate two adjacent wells simultaneously. Light irradiation was performed from above with the lid off. The three groups were on the edges of the plate and separated from each other to eliminate the effects of light scatter during treatment. Also a black mask was used to cover the wells that were not treated. The 980 nm wavelength laser had an aiming beam (650 nm wavelength, 3.5 mW output power on the high setting) that remained on during laser treatment. Therefore, an experimental group was included (aiming beam group) that was irradiated with the aiming beam only. These cells were treated the same as the 980 nm wavelength group except only the aiming beam was on

(irradiation time: 8 minutes and 20 seconds, power density: 0.01 mW/cm^2 and energy density: 5 mJ/cm^2).

MTS assay. At 40 minutes after irradiation, the MTS assay (Promega, Madison, WI) was performed to measure the metabolic activity of the cells. The test was performed according to the manufacturer's instruction and was duplicated for each combination of parameters. A series of tests were done to determine the optimal incubation time in the MTS solution. One hour and 30 minutes resulted in the best absorption reading. After incubation with MTS solution, the supernatant was removed for absorption reading at a wavelength of 492 nm.

Culture of primary rat cortical neurons. One well in a 2-well chamber slide was coated with 30 μg/ml Poly-D-Lysine and 2 μg/ml Laminin according to manufacture protocol. Rat cortical neurons (Lonza, Inc., Walkersville, MD) were thawed from liquid N_2 and seeded 8×10^3 cells/well in primary neuron growth medium (Lonza, Inc.) with glucose concentration of either 25 mM as control or 180 mM as high glucose level. Neurons were subjected to high glucose concentrations to cause impairment of their metabolism and neurite extension. The high glucose concentration was established in a preliminary study which found a 28% decrease of total neurite length ($P < 0.001$) when rat cortical neurons were cultured in 180 mM glucose compared to control (25 mM glucose) (Table 1).

Laser irradiation of rat cortical neurons. For comparison of the effects between 980 and 810 nm wavelength light, cells were irradiated with either a 980 nm CW laser (LiteCure, LLC; 1 W) or an 810 nm CW laser (Thor International, UK; 150 mW). The parameters for both lasers were power density of 10 mW/cm^2 and energy densities of 10, 50, 200, 1,000, and 5,000 mJ/cm^2. Cells were treated immediately after seeding and once again 24 hours later. Cells were fixed 24 hours after the second irradiation.

For further optimization of energy density for 980 nm wavelength light, a broader range of energy densities was studied. The parameters were 1 W output power, power density of 10 mW/cm^2, and energy densities of 0.01, 0.1, 0.5, 2, 10, 50, 200, 1,000, and 5,000 mJ/cm^2. A shutter controller (UNIBLITZ Corp., Rochester, NY) was placed in the path of light between the laser and chamber slide to control treatment time. The heights of the laser and shutter controller were adjusted so that the beam size was larger than the culture chamber (2 cm × 2 cm) and the power density on the cells was 10 mW/cm^2. Cells were treated immediately after seeding and again 24 hours later. Cells were fixed 24 hours after the second irradiation for further assessment.

Neurite assessment. The cells were fixed with 4% paraformaldehyde at 24 hours after the second irradiation. Each condition was duplicated. Images of all neurons (between 60 and 150 neurons in each group) were digitally photographed using an Olympus DP72 microscope digital camera (Olympus Imaging America, Inc., Center Valley, PA). The images of the neurons were uploaded to ImageJ with NeuronJ plugin (Version 1.45s). Neurites were counted for each neuron and neurite length was measured. Total neurite length was calculated as the sum of the length of all neurites from each neuron.

Temperature measurement. An infrared imaging system (FLIR Systems ThermoVision A40, moviMED, Irvine, CA) was used to detect temperature change in culture medium of the rat cortical neurons during irradiation. The computerized camera was focused on the culture dish without direct contact and temperature was recorded throughout the duration of the irradiation.

In Vivo Experiments

Animals. A total of 22 male White New Zealand rabbits (2.34–2.89 kg) were used in this study. The animal use protocol was reviewed and approved by the Uniformed Services University of the Health Sciences (USUHS) Institutional Animal Use Committee. Research was conducted in compliance with the Animal Welfare Act and other federal statutes and regulations relating to animals and experiments involving animals, and adhered to the principles stated in the Guide for the Care and Use of Laboratory Animals, National Research Council publication, 1996 edition.

Surgery. The rabbits were anesthetized with Ketamine/Xylazine (25 mg/kg: 5 mg/kg) and endo-tracheal intubation was performed. Anesthesia was maintained with isoflurane (3.0% with 1.5 L/minute O_2). Povidone iodine surgical scrub was used to clean the skin in the surgical area after shaving the hair. The skin was incised along the posterior

TABLE 1. In Vitro Cortical Neuron Neurite Length and Number

	In vitro cortical neurons		
Measurement	Control neurons 25 mM glucose	Impaired neurons 180 mM glucose	Decrease ratio (P value)
Total length (micron)	163.10 ± 5.89	118.00 ± 5.48	28% ($P < 0.001$)
Average length (micron)	45.94 ± 1.47	39.63 ± 1.67	14% ($P < 0.05$)
Neurite number	3.55 ± 0.11	2.98 ± 0.11	17% ($P < 0.01$)

Neurite extension was measured using ImageJ with NeuronJ Plugin. Measurements were analyzed by one-way ANOVA with Tukey's multiple comparison test. There was a 28% decrease in total neurite length, a 14% decrease in average neuron length, a 17% decrease in neurite number when rat cortical neurons were cultured in 180 mM glucose compared to control (25 mM glucose). Based on this data, total neurite length was used as the assessment measure for optimization of the laser treatment parameters for 980 nm wavelength light.

aspect of left thigh and the superficial fascia along the sciatic vein was sharply divided. The biceps muscle was bluntly dissected away from the semitendinous muscle and retracted laterally to fully expose the peroneal nerve. The left peroneal nerve was completely transected and sutured back together by end-to-end epineural suture using 8–0 Ethilon suture. Skin was closed using a buried running subcutaneous suture technique with 4–0 Monocryl suture and cleaned with sterile saline. The rabbits recovered in heated post-surgical recovery chambers before they were returned to their cages.

Light penetration measurements. Penetration of 980 nm wavelength light through the skin and femoral biceps muscle overlying the peroneal nerve was measured in two anesthetized, male White New Zealand rabbits. A near infrared power meter was designed and built by B&W Tek, Inc. (Newark, DE) to measure the power density (Fig. 3A,B) below the skin and at the level of the peroneal nerve. A small photo sensor (2.0 mm × 2.5 mm) was sealed in glass tube. The output voltage of the sensor was calibrated such that a reading of 1 mV represented a power density of 1 mW/cm^2. Surgery was done as described above to expose the peroneal nerve. The output power of the laser was set at 1.0 or 4.0 W. Power density measurements were taken at the surface of the skin, sub-dermally, and at the level of the peroneal nerve. Each measurement was done in triplicate and the average number was used for calculation of penetration.

Calculation of laser parameters used in pilot and long term studies. Based on our data from the *in vitro* experiments on rat cortical neurons, the optimal parameters for laser irradiation with 980 nm wavelength light were energy densities between 2 and 200 mJ/cm^2 at a power density of 10 mW/cm^2. Penetration measurements of 980 nm wavelength light to the level of the peroneal nerve in the living anesthetized rabbit revealed that approximately 2.45% (average of the 4.0 and 1.0 W measurements) of 980 nm wavelength light penetrated to the level of the nerve. To assure adequate treatments time for the *in vivo* experiments, calculations were based on the high end of the range of effective *in vitro* energy densities (200 mJ/cm^2). Therefore, the energy density needed at the surface of the skin would be (200 mJ/cm^2)/0.0245 = 8.16 J/cm^2. The treatment area necessary to cover the length of the injured peroneal nerve in the thigh was 8 cm^2 and the total energy delivered to this area based on an energy density of 8.16 J/cm^2 was 65 J. Therefore the 980 nm wavelength laser parameters used in the pilot study were: 2W group (output power: 2.0 W, irradiation time: 32 seconds, area: 8 cm^2, 65 J delivered over the area) and 4W group (output power: 4.0 W, irradiation time: 16 seconds, area: 8 cm^2, 65 J delivered over the area).

Based on the results of the pilot study, a power density of 10 mW/cm^2 at the level of the peroneal nerve was selected for the long-term study. To match a power density of 10 mW/cm^2 at the level of the nerve, 408 mW/cm^2 (10 mW/cm^2/0.0245 = 408 mW/cm^2) would be needed on the skin. The beam diameter was 2.2 cm or an area of 3.8 cm^2. Therefore, 408 mW/cm^2 × 3.8 cm^2 = 1.55 W. The closest output power setting on the laser was 1.5 W. To keep the total energy delivered at 65 J, the treatment time was 43 seconds and the treatment area was kept at 8 cm^2.

Pilot study. Eight White New Zealand rabbits underwent peroneal nerve transection followed by end-to-end epineural suture as described above. The rabbits were randomly placed into three groups (four rabbits for control and two rabbits per laser treatment group): Control (received no laser treatment), 2W group (980 nm wavelength, CW, output power: 2.0 W, treatment time: 32 seconds, 8 cm^2 area, 65 J) and 4W group (output power: 4.0 W, treatment time: 16 seconds, 8 cm^2 area, 65 J). Laser treatment was done once daily for 10 consecutive days starting immediately after surgery. The control group rabbits were treated exactly the same but the laser was off. The rabbits had been gentled and were held during the treatments. Two control rabbits were euthanized at 14 days post-surgery with sodium pentobarbital (150 mg/kg, IP) for silver stain analysis and six rabbits were euthanized at 21 days post-surgery for axonal immunolabeling.

Long term study. Twelve White New Zealand rabbits were randomized into 2 groups: control (no laser treatment) and LT (laser treatment group, laser treatment parameters: 980 nm wavelength, CW, output power: 1.5 W, treatment time: 43 seconds, and 8 cm^2 area, 65 J). Surgery was performed as in the pilot study. The left side of peroneal nerve was completely transected and then repaired using epineural suture. Light was applied immediately after closure of the skin. Daily irradiation was performed for 10 consecutive days. The control group was handled the same way as the light-treated group except the laser was off during treatment time. Rabbits were euthanized at 9 weeks post-surgery with sodium pentobarbital (150 mg/kg, IP).

Toe spread reflex test. The toe spread reflex test has been shown to be an effective measure of function for the peroneal dependent muscles of rabbit [9]. Briefly, rabbits were lifted in the air and suddenly lowered without letting them touch a surface. The injured animals lose the native reflex to spread the toes. The behavioral test was video recorded from the front of the animal so that the full width of both hind feet could be captured. The toe-spreading reflex test was performed at baseline and weekly starting from 4 weeks post-surgery. Images of the toe spread were extracted from the video and analyzed by ImageJ. The width of the feet were measured pre- and post-injury. The toe spread was calculated as a ratio of post-injury to pre-injury width on the left foot.

Silver stain. The peroneal nerves were harvested 14 days post-injury and fixed in 4% paraformaldehyde overnight. The nerves were then cryoprotected in 30% sucrose for 48 hours. Transverse sections (20 μm thickness) of the nerve samples from 1 cm proximal and 1 cm distal to injury site were cut using a cryostat. Selected sections were stained according to manufacturer's instructions using a modified Bielschowsky's stain kit (America Mastertech, Lodi, CA). The nerve sections were photographed using an Olympus BX50 microscope equipped

with a CellSens DP72 imaging camera (Olympus Imaging America, Inc.).

Immunolabeling of axons in pilot study. The peroneal nerves were dissected from the euthanized rabbits 21 days post-injury and fixed and cryoprotected as above. Transverse sections (10 μm thickness) of the nerve samples from 1 cm proximal and 2, 3, and 4 cm distal to injury site were cut using a cryostat. Immunohistochemistry was performed using antibody against protein gene product 9.5 (PGP9.5). Expression of PGP9.5 is highly specific to neurons and to cells of the diffuse neuroendocrine systems and stains regenerating neurons. Heat-induced antigen retrieval was first performed by soaking the slides in heated citrate buffer (pH 6.0) for 30 minutes. The sections were blocked with 10% normal goat serum in PBS for 15 minutes at room temperature. After incubating with primary antibody (Mouse anti-PGP9.5, AbD Serotec, Raleigh, NC) for 1 hour, secondary antibody (Alexa-Fluor488 Goat anti-mouse IgG, Life Technologies, Grand Island, NY) was used to visualize the antigen. The nerve sections were photographed and images digitally collected using an Olympus DP72 microscope digital camera (Olympus Imaging America, Inc.). The intensity of positive labeling was analyzed using ImageJ software.

Labeling of motor end plates in long term study. For the long-term study, the peroneal nerve related muscles from both left side (injured) and right side (uninjured) were collected and fixed in 4% paraformaldehyde overnight. The collected muscles included the Peroneus Brevis and Peroneus Tertius. The muscles were transferred to 30% sucrose for 48 hours. Serial 20 μm thick longitudinal sections were cut. Neurofilaments were immunolabeled to visualize the peroneal nerve axons. Sections were washed in PBS and blocked in 0.2% Triton, 10% goat serum in PBS for 30 minutes at room temperature, followed by overnight incubation with Mouse anti- Neurofilament 160/200 (NF160/200, Life Technologies, Corp., 1: 100 diluted in 1% goat serum, 0.2% Triton in PBS) at 4°C. After washing with 1% goat serum, 0.2% Triton in PBS, the sections were incubated for 1 hour with Goat anti-Mouse secondary antibody conjugated to Alexa Fluor 488 (Life Technologies, Corp. 1:300 diluted in 1% Goat serum, 0.2% Triton in PBS), and α-bungarotoxin (α-BTX) conjugated to Alexa Fluor 594 (Life Technologies, Corp., 2 μl/ml final concentration) at room temperature. α-BTX was used because it binds to acetylcholine receptors on muscle fiber. The main location of this receptor is on muscle end plates. After washing with PBS, slides were coverslipped with Vectashield mounting medium (Vectors Laboratories, Inc. Burlingame, CA) and sealed with nail polish. The images of motor endplates collected from the sections were uploaded to ImageJ (Version 1.45s) and the length of each motor endplate was measured. Motor end plates lengths are presented as mean ± SEM.

Statistical analyses. Statistical analyses were performed using GraphPad Prism (version 3.02, GraphPad Software, Inc., La Jolla, CA). MTS assay, neurite assessment and PGP9.5 immunolabeling were analyzed by one-way ANOVA with Tukey's multiple comparison test. The toe spread test were analyzed with repeated measures ANOVA with time as a within-subjects factor, groups (LT and control) as a between-subjects factor, and ratio to baseline as the dependent variable. Dunnett's multiple comparisons test was used to compare each time point to week 4 separately for each group, and Sidak's multiple comparisons test was used to compare groups at each time point. Familywise error rate was set at alpha = 0.05. The motor end plate data was analyzed by one-way ANOVA with Tukey's multiple comparison test. A statistically significant difference was defined as P value less than 0.05.

RESULTS

Primary Human Fibroblasts –MTS Assay

The effects of altering time of irradiation at a power density of 10 mW/cm^2 for two different wavelengths of light on *in vitro* human fibroblast mitochondrial metabolism are summarized in Figure 1. The laser had an aiming beam that remained on during laser treatment. Therefore, an experimental group was included (aiming beam group) which was irradiated with the aiming beam only. These cells were treated the same as the 980 nm wavelength group. There was no statistical difference in the mitochondrial metabolism of the non-treated controls and the fibroblasts treated with the aiming beam as measured by mitochondrial dehydrogenase activity using the MTS

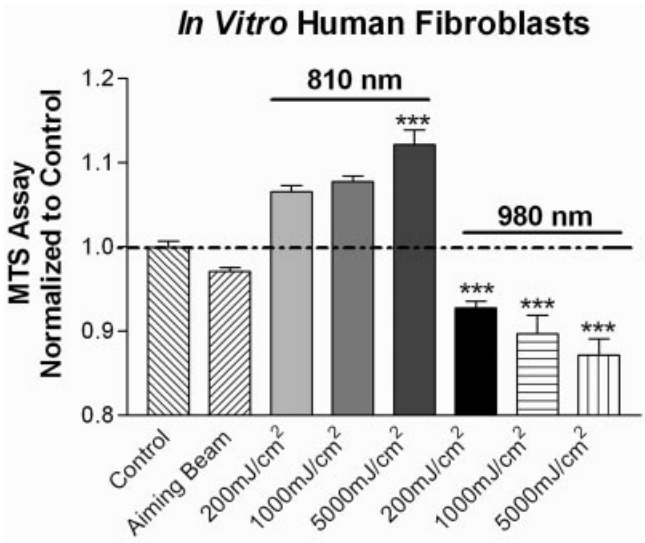

Fig. 1. Mitochondrial metabolism of *in vitro* human fibroblasts measured by the MTS assay. The fibroblasts were either not treated (Control), treated with the 650 nm wavelength aiming beam, or treated with 810 nm or 980 nm wavelength light. The data were normalized to the control data. There was no difference in the mitochondrial metabolism of the non-treated controls and the fibroblasts treated with the aiming beam. For the range of energy densities investigated, 810 nm wavelength light at an energy density of 5,000 mJ/cm^2 caused a statistically significant increase in mitochondrial metabolism. Over the same range of energy densities, 980 nm wavelength light caused a statistically significant decrease in mitochondrial dehydrogenase activity for all energy densities tested. $^{***}P < 0.001$. Bars represent the mean and the error bars represent the standard error of the mean.

assay. For the range of energy densities investigated, 810 nm wavelength light at an energy density of 5,000 mJ/cm^2 caused a statistically significant increase in mitochondrial metabolism. Over the same range of energy densities, 980 nm wavelength light caused a statistically significant decrease in mitochondrial dehydrogenase activity for all energy densities tested. This finding is important and illustrates that it cannot be assumed that laser parameters optimized for one wavelength can be used for other wavelengths.

Primary Rat Cortical Neurons—Total Neurite Length

To determine effective energy densities for 980 nm wavelength light, a series of experiments was done using *in vitro* rat cortical neurons. The neurons were subjected to high glucose concentrations to cause impairment of their metabolism and neurite extension. The glucose concentration used in these experiments was established in a preliminary study in which it was found that a 28% decrease of total neurite length ($P < 0.001$), a 14% decrease in average neuron length ($P < 0.05$), and a 17% decrease in neurite number ($P < 0.01$) occur when rat cortical neurons were cultured in 180 mM glucose compared to control (25 mM glucose) (Table 1).

Our experiments using *in vitro* human fibroblasts indicated that lower energy densities of 980 nm wavelength light may be required compared to 810 nm wavelength light for a specific power density. Therefore, for the first experiment determining effects of 810 or 980 nm wavelength light on total neurite extension of neurons cultured in 180 mM glucose compared to the control neurons grown in 180 mM glucose or 25 mM glucose, a lower range of energy densities (10, 50, 200, 1,000, and 5,000 mJ/cm^2) was examined at a power density of 10 mW/cm^2. For cortical neurons subjected to high glucose concentration, 980 nm wavelength light significantly promoted neurite extension at energy densities of 10 and 50 mJ/cm^2 compared to the control neurons cultured in 180 mM glucose (Fig. 2A). These data led us to examine a broader range of low energy densities of 980 nm wavelength light at a power density of 10 mW/cm^2 (Fig. 2B). Also the sample size for the total neurite length measurements was increased from an N of 60 to an N of 150. The 980 nm wavelength light significantly promoted total neurite extension at energy densities of 2, 10, 50, and 200 mJ/cm^2 (Fig. 2B).

An infrared imaging camera was used to detect temperature change in the rat cortical neuron cultures during irradiation (Fig. 2B) to determine if there was a thermal component to the effect. A temperature rise of approximately 0.1°C was found beginning with an energy density of 1,000 mJ/cm^2 and increased to approximately 0.7°C at an energy density of 5,000 m J/cm^2. It is important to note that these fluences did not support neurite elongation. Therefore the significant increases in total neurite at fluences of 2, 10, 50, and 200 mJ/cm^2 could not be attributed to a thermal effect but to a photobiological effect. These data indicate that lower energy densities of 980 nm wavelength light were required compared to 810 nm wavelength light for a specific power density.

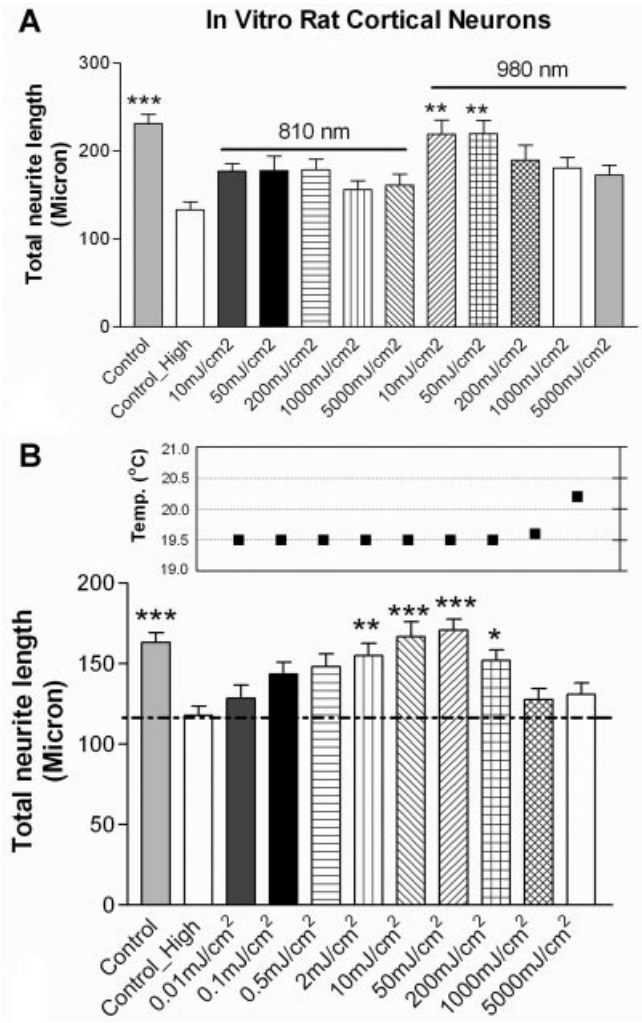

Fig. 2. Graphs showing effective energy densities for 810 and 980 nm wavelength light based on total neurite length of *in vitro* rat cortical neurons cultured in 180 mM glucose. **A**: Nine-hundred eighty nanometer swavelength light significantly promoted neurite extension at energy density of 10 and 50 mJ/cm^2 compared to the control neurons cultured in 180 mM glucose. **B**: A broader range of low energy densities of 980 nm wavelength light at a power density of 10 mW/cm^2 were tested and energy densities of 2, 10, 50, and 200 mJ/cm^2 significantly promoted total neurite extension. A temperature rise of approximately 0.1°C was found beginning with an energy density of 1,000 mJ/cm^2 and increased to approximately 0.7°C at an energy density of 5,000 mJ/cm^2. $^*P$ of 0.01 to 0.05, $^{**}P$ of 0.001 to 0.01, $^{***}P < 0.001$. Bars represent the mean and the error bars represent the standard error of the mean.

Penetration of 980 nm Wavelength Laser

Penetration of the 980 nm wavelength light through the skin and femoral biceps muscle overlying the peroneal nerve was measured in an anesthetized rabbit. Surgery was performed to expose the peroneal nerve by retracting the skin and femoral biceps muscle. The power meter was placed sub-dermally; or under skin and muscle (Fig. 3A), with the sensor positioned on the surface of the nerve

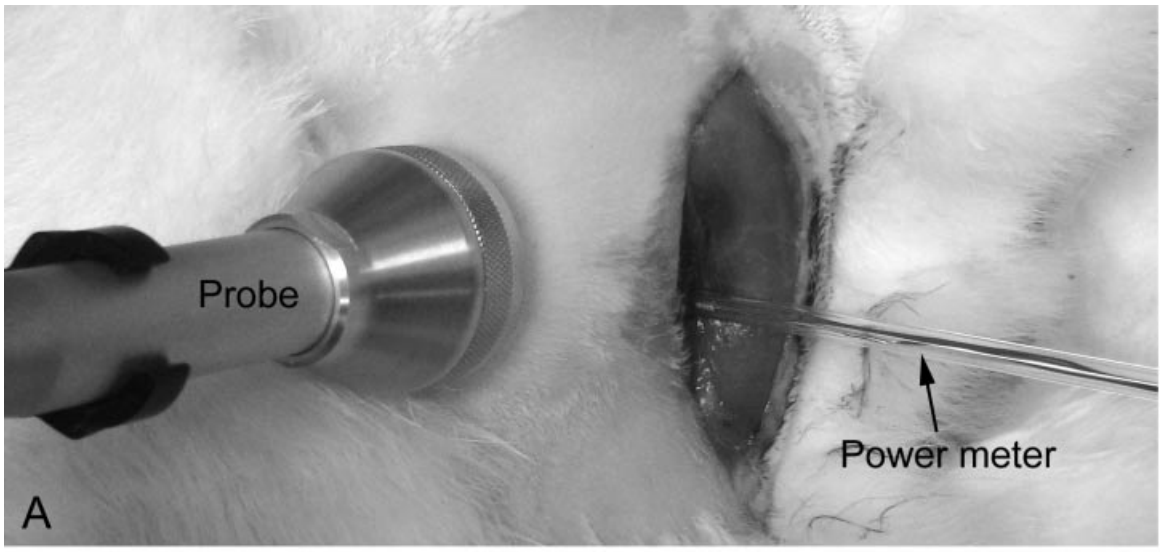

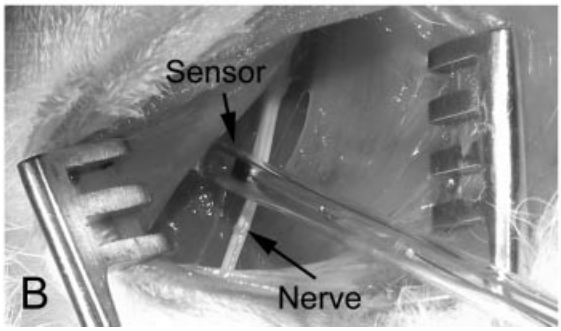

C

Output power	1 W	4 W
	Power Density	
At skin surface	1.8 W/cm^2	7 W/cm^2
Sub-dermal	0.6 W/cm^2	2.1 W/cm^2
Level of Nerve	34 mW/cm^2	200 mW/cm^2

Fig. 3. In vivo measurement of light penetration in an anesthetized rabbit. **A**: The photograph shows the experimental set up. The power meter is inserted into the incision and the laser probe is placed in contact with the shaved skin. **B**: In this photograph, the peroneal nerve can be see coursing below femoral biceps muscle. The small photo sensor (2 mm × 2.5 mm) in the glass tube is placed on top of peroneal nerve. **C**: Table listing the power densities measured at the skin surface, sub-dermally and at the level of the nerve at output powers of 1 and 4 W.

(Fig. 3B). In this region, the skin and muscle had a thickness of 1 and 11 mm, respectively. The light penetrated to the depth of the peroneal nerve. At an output power of 1.0 W and a power density on the skin surface of 1.8 W/cm^2, the power density was 0.6 W/cm^2 sub-dermally, and 34 mW/cm^2 at the level of the nerve (Fig. 3C). At an output power of 4.0 W and a power density on the skin surface of 7.0 W/cm^2, the power density sub-dermally was 2.1 W/cm^2, and 200 mW/cm^2 at the level of the nerve (Fig. 3C). Therefore 30% of the power density delivered to the skin surface penetrated through the skin for both output powers settings (1.0 and 4.0 W). With a 1.0 W output power, 1.9% of the power density delivered to the skin penetrated to the level of the nerve while with a 4.0 W output power, 2.9% penetrated to the level of the nerve.

Pilot Study

Gross observation of the injury site at 14 days post-injury revealed that there was reattachment of the ends of the transected peroneal nerve and an enlargement of the area (Fig. 4A). Silver staining of the transected nerve revealed significant degenerative changes (Fig. 4B and C). A comparison of sections 1 cm proximal to the lesion site (Fig. 4B) and 1 cm distal to the lesion site (Fig. 4C), showed an almost complete degeneration of the axons and their associated myelin at 1 cm distal to the lesion site. Fine granular and/or brown stained material was present in the areas bounded by the epineurium indicating the last stages of Wallerian degeneration (Fig. 4C). The majority of the circular epineurial profiles were completely empty. Also a few of the epineurial profiles contained a normal staining axon indicating that a few neurons are beginning the regenerative process. These axons are not myelinated since that occurs at a later stage of regeneration (Fig. 4C). Analysis of the density of immunolabeling for PGP9.5, revealed that at 21 days post-injury there was significantly less labeling in the 4W group than control and 2W groups ($P < 0.001$) at 3 and 4 cms distal to the transaction site (Fig. 4D–F). These data show that 4W laser parameters inhibited

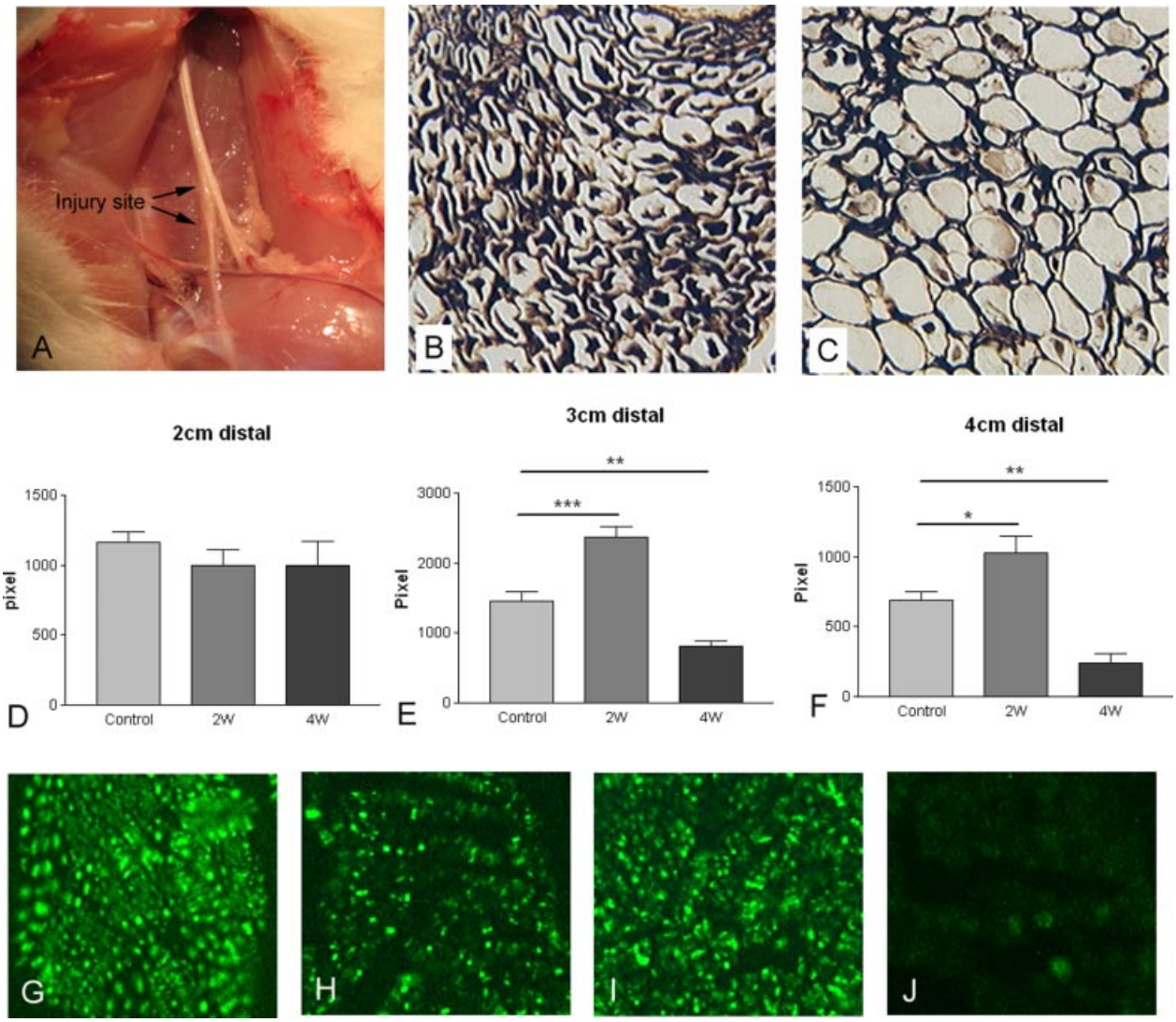

Fig. 4. Pilot study results. **A**: Injury site at 14 days post-injury (indicated by arrows). **B**,**C**: Silver stained peroneal nerve samples 14 days after transection injury. B: Photomicrographs of the nerve 1 cm proximal to the injury site and (C) 1 cm distal to the injury site. The density of PGP9.5 immunolabeling was analyzed at 2 cm (**D**), 3 cm (**E**), and 4 cm (**F**) distal to the transection site at 21 days post-injury. There was significantly less labeling in the 4W group than control and 2W groups ($P < 0.001$) at 3 and 4 cm distal to the transection site (E,F). Photomicrographs of PGP9.5 antigen visualized by the green fluorescence label in peroneal nerve at 14 days post-injury: (**G**) 1 cm proximal to the transection site, (**H**–**J**) 4 cm distal to the transection site for (H) Control, (I) 2 W, (J) 4 W $^{*}P$ of 0.01 to 0.05, $^{**}P$ of 0.001 to 0.01, $^{***}P < 0.001$. Bars represent the mean and the error bars represent the standard error of the mean.

nerve regeneration. Too much light energy has been shown to be inhibitory to a wide variety of cellular processes. At 2 cm post-lesion there was no significant difference between the control and the 2 laser treatments. At 3 and 4 cm distal to the injury site, the 2W laser treatment had significantly better axonal regeneration than the control. It is important to note that in our rabbit model, the distance from the lesion site on the peroneal nerve to the muscles in the foot innervated by the peroneal nerve was 240–280 mm. It has been reported that the average rate of regeneration of motor axons of the peroneal nerve after transection and suturing was approximately 2 mm a day [10]. Since the survival time was only 3 weeks in this pilot study, improvement in function was not expected for the control and light treated nerves because at 3 weeks the nerves would have regenerated only in the 3 to 6 cm range. Schmitz and Beer [9] reported that the earliest the onset of peroneal nerve motor recovery as detected by the toe spread reflex was 9 weeks post injury.

Long Term Study: Toe Spread Reflex Test

Rabbits with a complete, unilateral, peroneal nerve transection were used for the long-term study. The LT group had irradiation for 10 consecutive days post-surgery. The toe spread reflex behavior test was performed before surgery as a baseline (Fig. 5A) and weekly beginning at 4 weeks post-surgery. At week 4, the mean toe spread decreased to $63.7 \pm 2.6\%$ and $68.2 \pm 3.8\%$ of baseline for control and LT groups respectively (Fig. 5B,D), which indicated functional loss in both groups. There was no significant functional recovery in either the LT or control groups at week 5 and 6 post-injury. At weeks 7, 8, and 9, the LT group showed statistically significant functional recovery compared to week 4 ($P < 0.001$). Multiple comparisons of each time point to week 4 in the control group did not show any functional recovery (Fig. 5D). The LT group consistently performed significantly better in the toe spread reflex test compared to the control group starting from week 7, with a return of function to $89.1 \pm 4.0\%$ in the LT group and $72.2 \pm 3.6\%$ in the control group ($P < 0.05$) by week 9 (Fig. 5C,D). The significant improvement in the LT group demonstrated that light treatment promoted earlier and faster nerve regeneration and functional recovery.

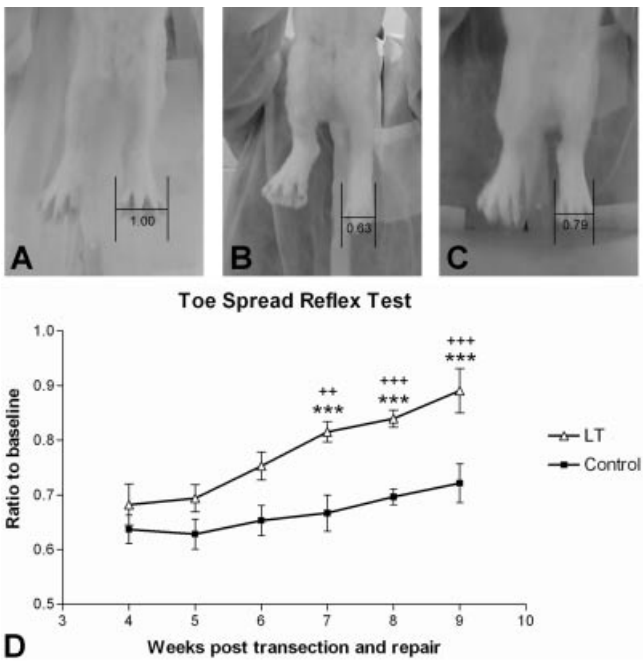

Fig. 5. Behavior assessment: toe spread reflex test. **A–C**: Representative photographs showing the toe spread reflex of a rabbit from the light treated group at baseline (A), 4 weeks post-surgery (B), and 9 weeks post-surgery (C). Toe spread was measured as pixel length across the widest part of the toes using ImageJ. The ratio to baseline (indicated by the number below the measurement bars) was calculated by dividing post-injury width by the pre-injury width. **D**: The results of the toe spread reflex test (ratio to baseline) from weeks 4 to 9 post-injury for the LT group and the non-treated control group (Control). The asterisks indicate significant difference between each week and week 4 for either LT or control groups. $^{***}P < 0.001$. The plus signs indicate significant difference between LT and control groups on each week. $^{++}P < 0.01$, $^{+++}P < 0.001$. Bars represent the mean and the error bars represent the standard error of the mean.

Assessment of Motor Endplates

The length of motor endplates in sections of the Peroneal Tertius and Brevius muscles were measured (Fig. 6). The motor endplates were visualized by labeling with α-BTX conjugated to Alexa Fluor 594. Motor endplate length is directly related to whether it is innervated or deinnervated. The average length of the motor endplates in the muscles innervated by the peroneal nerve on the right side (uninjured) was 17.36 ± 0.26 μm. The average motor endplate length decreased to 11.20 ± 0.72 μm at 9 weeks post-injury while the average motor endplate length on the injured and light treated side (16.94 ± 0.52 μm) returned to uninjured levels. These data indicate that light irradiation supported peroneal nerve regeneration and reinnervation of the involved muscles by 9 weeks post-injury.

DISCUSSION

Numerous peer reviewed studies have established the efficacy of PBM for treatment of peripheral nerve injury. Reviews of the relevant literature demonstrate that different wavelengths can support peripheral nerve injury repair. The majority of the wavelengths used in these studies were in the 600–904 nm range [6,7]. Wavelengths longer than 904 nm typically have not been used for peripheral nerve repair and their effects in promoting peripheral nerve regeneration have not been adequately researched. Recently, 940 nm wavelength irradiation was used to treat a crush injury of the rat sciatic nerve [11]. The results were positive with a reported reduction in edema and inflammation and increased functional recovery on post-injury days 7, 14, and 21 based on the sciatic function index (SFI).

A key issue in the field of PBM is the lack of parameter optimization. Preliminary studies to optimize the treatment parameters are rarely done. A few studies have attempted to compare the efficacy of two or more wavelengths for peripheral nerve injury repair. In these experiments, the same parameters were used for both wavelengths without regard for differences in wavelength penetration to the target tissue or optimization of the parameters for each wavelength [12,13]. Barbosa et al. [10] examined the comparative effects of 660 and 830 nm wavelength light on crush injury of the rat sciatic nerve. The parameters used for both wavelengths included an output power of 30 mW and 10 J/cm^2 on the skin surface. The 660 nm wavelength light resulted in improved functional recovery on day 14. No statistical difference was seen between the sham, 660 nm wavelength group and 830 nm wavelength group at 7 days or 21 days. The authors concluded that the 660 nm wavelength used with these parameters was more effective than 830 nm wavelength light. However, a significant difference at only one time point examined suggests that the parameters used for both wavelengths were not optimal. The effects of 660 and 780 nm wavelength light on neuromuscular and functional

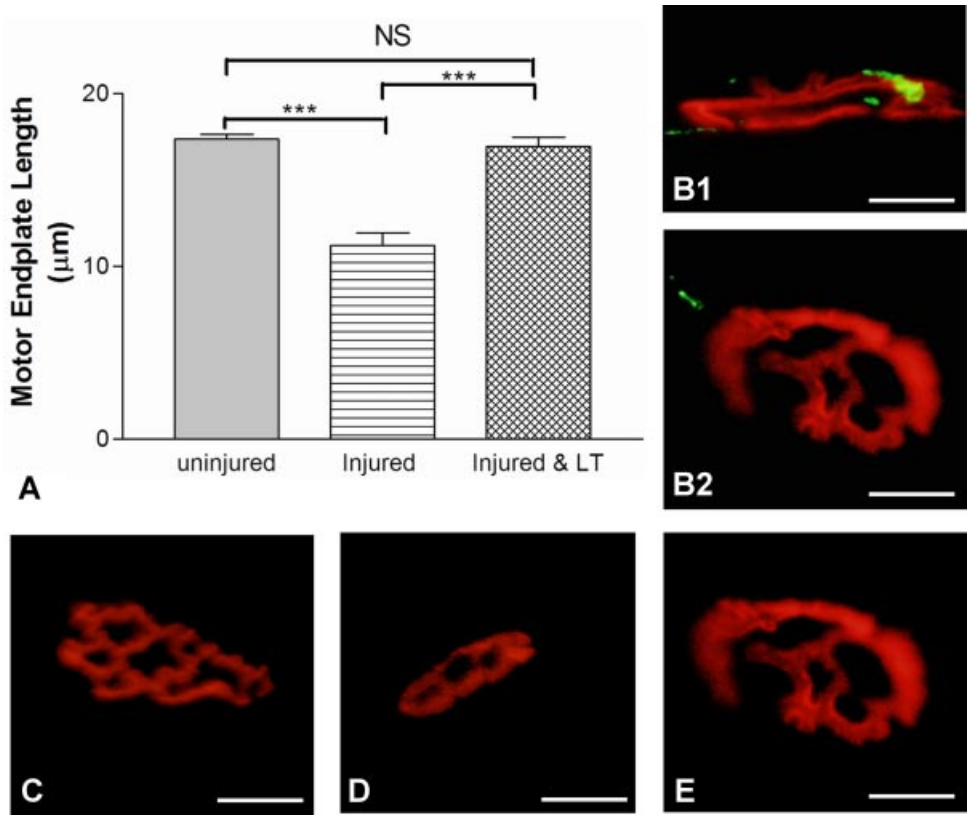

Fig. 6. Motor endplate measurement and labeling. **A**: Graph showing means of motor endplate length (μm) for the uninjured (right side), injured, and injured and LT (left side) groups. Measurement of motor endplate length tested by one way ANOVA with Tukey's multiple comparison test showed significant difference between uninjured and injured ($^{***}P < 0.001$) and injured LT and injured ($^{***}P < 0.001$) groups. (**B1**–**B2**) Motor endplates from the Peroneal Tertius and Brevius muscles of rabbits at 9 weeks after nerve transection and LT (red, labeled with α-BTX conjugated to Alexa Fluor 594) innervated by immunolabeled peroneal nerve (green). **C**,**D**,**E**: Labeled motor endplates: (C) from the uninjured side (right) of the rabbit, (D) from injured left side of the rabbit with peroneal nerve transection, (E) from a rabbit that had nerve transection and light therapy. Bars represent the mean and the error bars represent the standard error of the mean. Scale bar = 10 μm.

recovery were investigated using a crush injury model of the rat sciatic nerve [13]. The same laser parameters were used for both wavelengths. Neither wavelength improved function and suggests that the laser parameters for both wavelengths were not optimal.

There is one report in the literature on PBM treatment of peripheral nerve injury in which laser parameters were used in an animal model and then translated to the human [14,15]. Light, 780 nm wavelength, was used to treat severe sciatic nerve injury in a rat model [14] and in a human randomized double-blind placebo-controlled study of long term incomplete peripheral nerve injury [15]. The laser parameters used in the rodent study were 780 nm wavelength light, output power 200 mW, 15 minutes transcutaneous treatments over the reconstructed sciatic nerve and the corresponding spinal cord segments, daily for 14 days [14]. Spot size was not reported so neither energy density nor power density could be calculated and compared to the non-effective parameters used for 780 nm wavelength light in the Gigo-Benato et al. study [13]. These treatment parameters resulted in an increased total number of myelinated axons and improved motor function based on the SFI behavior test [14]. The laser parameters used in the human trial were 780 nm wavelength light, output power 250 mW, 3-hour transcutaneous treatments over the injured peripheral nerve (450 J/mm^2) and 2 hours to the corresponding spinal cord segments (300 J/mm^2, spot size 6 mm^2) daily for 21 days [15]. The authors reported that there was accelerated nerve regeneration and a progressive improvement in motor nerve function over a 6-month period. No explanation was given for the selection of the parameters used in either the animal study or the clinical trial or how the clinical trial parameters related to those used in the rodent study. Furthermore, the nerves treated in the patients in the laser treated group included the median, ulnar, radial peroneal, axillary nerves, and the upper trunk of the brachial plexus. All these nerves were transcutaneously treated with the same laser parameters regardless of the depth of the nerve. Even though a

positive outcome was reported it is unlikely that optimization of the laser parameters was achieved.

There is no clear consensus on what wavelength may be best to use for a specific nerve and what parameters should be used for that wavelength. This lack of parameter optimization is responsible for the variability in results across studies and which is a criticism of PBM. As recently suggested [16], it is unreasonable to expect that a single light dose will have a universal application. However, many wavelengths may be efficacious for treatment of nerve injury if the wavelength can penetrate to the target tissue and the parameters used are optimized so that a therapeutic dose of light is applied.

For the majority of PBM studies, dose parameters reported were values delivered to the skin surface and not what was actually delivered to the target tissue. Our laboratory was the first to measure light penetration in an anesthetized rat from the dermis to the depth of the spinal cord using a smart, tissue-activated optical fiber probe attached to a spectrophotometer [17]. We also investigated the effect of PBM on peripheral nerve regeneration and function after severe median nerve injury and microsurgical autologous nerve graft repair using fibrin glue [18]. For these experiments, the percentage of output power of an 810 nm wavelength laser transcutaneously transmitted to the depth of the median nerve was measured in an anesthetized rat. Power transmitted through the skin to the depth of the nerve was 47% of the output power. Based on these measurements, laser parameters were chosen so that a power density of 10 mW/cm^2 was achieved at the depth of the nerve. Laser treatment with these parameters resulted in faster functional recovery of grip strength ($P < 0.05$), shorter compound muscle action potential latency ($P < 0.05$), and higher S-100 immunoreactivity ($P = 0.0213$).

Based on our data from the *in vitro* experiments on rat cortical neurons, the optimal parameters for infrared laser irradiation were energy densities between 2 and 200 mJ/cm^2 at a power density of 10 mW/cm^2. To assure adequate treatment time for the *in vivo* experiments, calculations were based on the high end of the range of effective *in vitro* energy densities (200 mJ/cm^2). The data from the penetration experiments of 980 nm wavelength light revealed that approximately 2.45% (average of 4.0 W and 1.0 W measurement) of the light penetrated to the level of the peroneal nerve. The total energy delivered on the skin surface was calculated to be 65 J. Two different output powers (2 and 4 W) were used for the pilot study. Although the total energy was kept at 65 J for both groups, nerve regeneration was significantly better with the 2 W laser treatment compared to the control while regeneration of the injured nerves was inhibited when treated with 4 W. Therefore, both energy density (200 mJ/cm^2) and power density (10 mW/cm^2) were considered for refining the calculation for the long-term study. Based on the toe spread reflex, these laser treatment parameters promoted an earlier and faster nerve regeneration and functional recovery compared to the non-treated controls and supported nerve regeneration and reinnervation of the involved muscles by 9 weeks post-injury.

Comparison between 980 and 810 nm wavelength light was done with two *in vitro* models. The experiments using human fibroblasts demonstrated that inhibition of mitochondrial metabolic activity was caused by 980 nm wavelength light, at 10 mW/cm^2 and energy densities that were stimulatory to mitochondrial metabolic activity with 810 nm wavelength light. In the cortical neuron experiments, 980 nm wavelength light at 10 mW/cm^2 and lower energy densities supported neurite elongation while at 10 mW/cm^2 and comparable energy densities 810 nm wavelength light had no effect on neurite elongation. These data demonstrate that for a given power density 980 nm wavelength light altered cellular activity at lower energy densities compared to 810 nm wavelength light. Thus, for different wavelengths of light at a given power density, the energy density necessary to achieve a desired effect may be very different.

This study demonstrates that treatment parameters for a specific wavelength of light can be determined initially using in *vitro* models and that these parameters can be translated to animal model research and clinical practice. The translation of dose from *in vitro* to *in vivo* was accomplished by first determining the effective laser parameters at the cellular level. The *in vitro* neuronal model used in this study involved compromised neurite elongation and not transection injury which was used in the *in vivo* animal model. Although the *in vitro* and *in vivo* models differed, the results demonstrate that optimizing the *in vitro* neuronal response to light at the cellular level provided a valid approach for the initial step in parameter optimization. The *in vitro* dose was then adjusted based on light penetration measurements. These results also validate that infrared light with optimized parameters is affective for treatment of nervous system injuries.

ACKNOWLEDGMENT

This research was funded by the Comprehensive National Neuroscience Program, Grant # G1704T. The opinions and assertions contained herein are the private ones of the authors and are not to be construed as official or reflecting the views of the Department of Defense or the Uniformed Services University of the Health Sciences.

REFERENCES

1. Bellamkonda RV. Peripheral nerve regeneration: An opinion on channels, scaffolds and anisotropy. Biomaterials 2006; 27(19):3515–3518.
2. Lundborg G. A 25-year perspective of peripheral nerve surgery: Evolving neuroscientific concepts and clinical significance. J Hand Surg Am 2000;25(3):391–414.
3. Evans GR. Challenges to nerve regeneration. Semin Surg Oncol 2000;19(3):312–318.
4. Hart AM, Terenghi G, Wiberg M. Neuronal death after peripheral nerve injury and experimental strategies for neuroprotection. Neurol Res 2008;30(10):999–1011.
5. Anders JJ, Geuna S, Rochkind S. Phototherapy promotes regeneration and functional recovery of injured peripheral nerve. Neurol Res 2004;26(2):233–239.
6. Gigo-Benato D, Geuna S, Rochkind S. Phototherapy for enhancing peripheral nerve repair: A review of the literature. Muscle Nerve 2005;31(6):694–701.
7. Rochkind S, Geuna S, Shainberg A. Chapter 25: Phototherapy in peripheral nerve injury: Effects on muscle preservation and nerve regeneration. Int Rev Neurobiol 2009;87:445–464.

8. Anders J, Romanczyk T, Ilev I, Moges H, Longo L, Wu X, Waynant R. Light supports neurite outgrowth of human neural progenitor cells in vitro: The role of P2Y receptors. IEEE J Selected Topics Quantum Electron 2008;14(1):118–125.
9. Schmitz HC, Beer GM. The toe-spreading reflex of the rabbit revisited–functional evaluation of complete peroneal nerve lesions. Lab Anim 2001;35(4):340–345.
10. Gutmann E, Guttmann L, Medawar P, Young J. The rate of regeneration of nerve. J Exp Biol 1942;19:14–44.
11. Serafim KG, Ramos Sde P, de Lima FM, Carandina M, Ferrari O, Dias IF, Toginho Filho Dde O, Siqueira CP. Effects of 940 nm light-emitting diode (led) on sciatic nerve regeneration in rats. Lasers Med Sci 2012;27(1):113–119.
12. Barbosa RI, Marcolino AM, de Jesus Guirro RR, Mazzer N, Barbieri CH, de Cassia Registro Fonseca M. Comparative effects of wavelengths of low-power laser in regeneration of sciatic nerve in rats following crushing lesion. Lasers Med Sci 2010;25(3):423–430.
13. Gigo-Benato D, Russo TL, Tanaka EH, Assis L, Salvini TF, Parizotto NA. Effects of 660 and 780 nm low-level laser therapy on neuromuscular recovery after crush injury in rat sciatic nerve. Lasers Surg Med 2010;42(9):673–682.
14. Rochkind S, Leider-Trejo L, Nissan M, Shamir MH, Kharenko O, Alon M. Efficacy of 780-nm laser phototherapy on peripheral nerve regeneration after neurotube reconstruction procedure (double-blind randomized study). Photomed Laser Surg 2007;25(3):137–143.
15. Rochkind S, Drory V, Alon M, Nissan M, Ouaknine GE. Laser phototherapy (780 nm), a modality new in treatment of long-term incomplete peripheral nerve injury: A randomized double-blind placebo-controlled study. Photomed Laser Surg 2007;25(5):436–442.
16. Arany PR. Photobiomodulation: Poised from the fringes. Photomed Laser Surg 2012;30 9: 507–509.
17. Byrnes KR, Waynant RW, Ilev IK, Wu X, Barna L, Smith K, Heckert R, Gerst H, Anders JJ. Light promotes regeneration and functional recovery and alters the immune response after spinal cord injury. Lasers Surg Med 2005;36(3):171–185.
18. Moges H, Wu X, McCoy J, Vasconcelos OM, Bryant H, Grunberg NE, Anders JJ. Effect of 810 nm light on nerve regeneration after autograft repair of severely injured rat median nerve. Lasers Surg Med 2011;43(9):901–906.